

Layout Sequence Prediction From Noisy Mobile Modality

Haichao Zhang
zhang.haich@northeastern.edu
Northeastern University
Boston, Massachusetts, USA

Yi Xu
xu.yi@northeastern.edu
Northeastern University
Boston, Massachusetts, USA

Hongsheng Lu
hongsheng.lu@toyota.com
Toyota Motor North America
Mountain View, California, USA

Takayuki Shimizu
takayuki.shimizu@toyota.com
Toyota Motor North America
Mountain View, California, USA

Yun Fu
yunfu@ece.neu.edu
Northeastern University
Boston, Massachusetts, USA

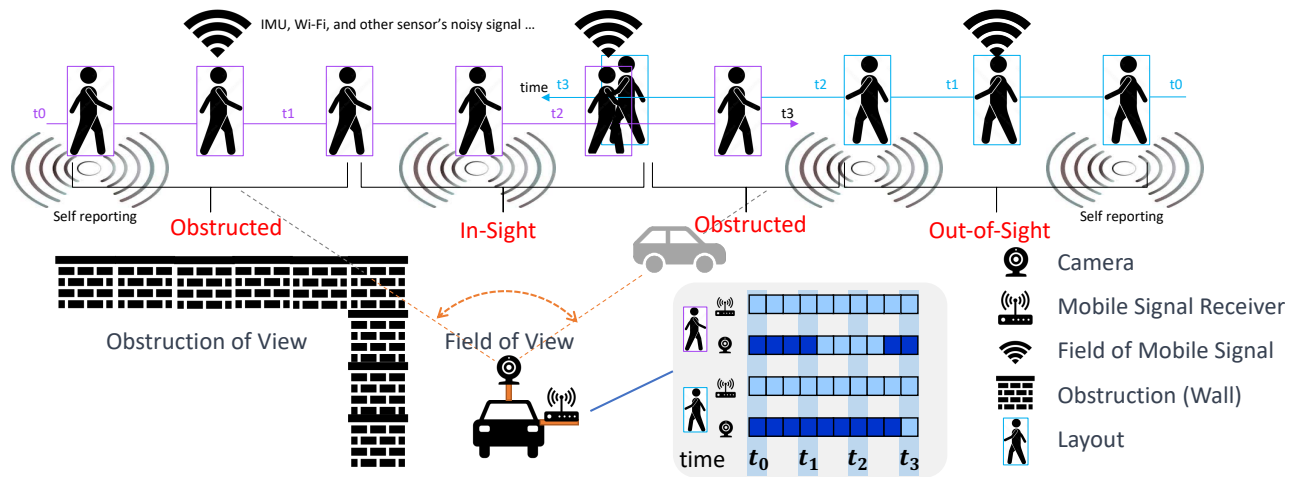


Figure 1: Illustration of a typical real-world scenario where a camera-equipped car captures the visual layout sequences and wireless mobile signals from pedestrians and cars. The orange line represents the camera's field of view, while the wireless icon indicates the mobile signal coverage. The figure demonstrates how obstacles, such as walls and cars, can obstruct the view of the camera and disrupt the mobile signals. For example, the pedestrian in the purple bounding box is obstructed by walls and a car before being captured by the camera, and the pedestrian in the blue bounding box walks out of the camera's view and is obstructed by a car. Meanwhile, their mobile sensor's signal remains within the field of reception during this process. The bottom right figure in grey area shows the "visibility" of the pedestrians in the black car's view of the visual and mobile modalities, in which dark color means invisible and light color means visible.

ABSTRACT

Trajectory prediction plays a vital role in understanding pedestrian movement for applications such as autonomous driving and robotics. Current trajectory prediction models depend on long, complete, and accurately observed sequences from visual modalities. Nevertheless, real-world situations often involve obstructed cameras, missed objects, or objects out of sight due to environmental factors, leading to incomplete or noisy trajectories. To overcome these limitations, we propose **LTrajDiff**, a novel approach that treats

objects obstructed or out of sight as equally important as those with fully visible trajectories. **LTrajDiff** utilizes sensor data from mobile phones to surmount out-of-sight constraints, albeit introducing new challenges such as modality fusion, noisy data, and the absence of spatial layout and object size information. We employ a denoising diffusion model to predict precise layout sequences from noisy mobile data using a coarse-to-fine diffusion strategy, incorporating the Random Mask Strategy, Siamese Masked Encoding Module, and Modality Fusion Module. Our model predicts layout sequences by implicitly inferring object size and projection status from a single reference timestamp or significantly obstructed sequences. Achieving state-of-the-art results in randomly obstructed experiments, our model outperforms other baselines in extremely short input experiments, illustrating the effectiveness of leveraging noisy mobile data for layout sequence prediction. In summary, our approach offers a promising solution to the challenges faced by layout sequence and trajectory prediction models in real-world settings, paving the way for utilizing sensor data from mobile phones

Permission to make digital or hard copies of all or part of this work for personal or classroom use is granted without fee provided that copies are not made or distributed for profit or commercial advantage and that copies bear this notice and the full citation on the first page. Copyrights for components of this work owned by others than the author(s) must be honored. Abstracting with credit is permitted. To copy otherwise, or republish, to post on servers or to redistribute to lists, requires prior specific permission and/or a fee. Request permissions from permissions@acm.org.

MM '23, October 29–November 3, 2023, Ottawa, ON, Canada

© 2023 Copyright held by the owner/author(s). Publication rights licensed to ACM.

ACM ISBN 979-8-4007-0108-5/23/10...\$15.00

<https://doi.org/10.1145/3581783.3611936>

to accurately predict pedestrian bounding box trajectories. To the best of our knowledge, this is the first work that addresses severely obstructed and extremely short layout sequences by combining vision with noisy mobile modality, making it the pioneering work in the field of layout sequence trajectory prediction.

CCS CONCEPTS

• **Computing methodologies** → **Motion path planning; Vision for robotics; Neural networks.**

KEYWORDS

Layout Sequence, Trajectory Prediction, Mobile Modality, Denoise, Diffusion Model, Out-of-Sight Problem, Modality Fusion

ACM Reference Format:

Haichao Zhang, Yi Xu, Hongsheng Lu, Takayuki Shimizu, and Yun Fu. 2023. Layout Sequence Prediction From Noisy Mobile Modality. In *Proceedings of the 31st ACM International Conference on Multimedia (MM '23)*, October 29–November 3, 2023, Ottawa, ON, Canada. ACM, New York, NY, USA, 9 pages. <https://doi.org/10.1145/3581783.3611936>

1 INTRODUCTION

Trajectory prediction is a critical problem in numerous research fields, including computer vision, robotics, mobile computing, and autonomous driving. The ability to predict future trajectories has the potential to significantly enhance the capacity of these fields to learn human behavior, make informed decisions for vehicles, and pedestrian collision detection. However, due to the intricate nature of application scenarios, this has remained a long-standing challenging problem. Although many works have greatly advanced this field, existing works often assume that the input signals are uncovered, accurate, long, and complete trajectories captured by cameras and estimated by computer vision algorithms, which is too strong an underlying assumption in practice.

Due to the prosperity of computer vision research, numerous topics have attempted to solve this problem and have achieved plausible performances, such as trajectory prediction, object tracking, and video frame prediction. These works have achieved great success in predicting accurate trajectories due to the high accuracy of computer vision algorithms. However, these works share an underlying assumption that relies heavily on the camera to capture the input data. Cameras have limited observation sight, which leads to difficulty in blind spots, cover issues, and out-of-sight problems. These limitations greatly impact real-world applications, for example, shortening the reaction time of autonomous driving algorithms and increasing the cost of deploying multi-camera systems for larger sight. Therefore, it is important to explore alternative approaches that can overcome these limitations and produce reliable results in real-world scenarios.

However, less attention pays to the mobile modality that has no out-of-sight problem to estimate the location and motion status of objects without concerns about out-of-view problems. With the development of mobile computing, sensors are now ubiquitous, including IMU mobile sensors [4, 12, 22, 27], wireless signals [26, 35], GPS [1, 10], satellite data, and user reports to provide out-of-view [5, 28] and blind area [7, 16] trajectory information. These sensors have no out-of-sight problem and can be received through a long range

without showing in the camera, which is much more ideal than the camera data in the visual modality. Moreover, computer vision algorithms also face challenges in dealing with occlusions and object appearance changes, which can lead to inaccurate bounding box predictions. In contrast, using sensor data to estimate object location and motion status can provide a complementary approach to improve the accuracy of bounding box prediction.

Despite these beneficial characteristics, there are two main challenges in leveraging mobile modality. The first is that the mobile modality often introduces noise [1, 3, 10, 23] that makes it difficult to extract accurate signals, particularly when compared to computer vision methods [25]. Another challenge is that important information, such as object size and other detailed information contained in the bounding box, is often missing in these signals, increasing the difficulty of making decisions for high-level tasks like scene understanding. Nevertheless, exploring the use of mobile modality alongside computer vision methods could lead to more accurate and reliable predictions of layout sequence in real-world scenarios. By combining the strengths of both modalities, we can potentially overcome the limitations of each and achieve more robust and efficient solutions.

To address these challenges, we propose a novel approach that combines the strengths of both visual and mobile modalities, aiming to predict a long sequence of layout points from a noisy mobile sensor's data sequence while conditioning on an extremely short or randomly obstructed input visual location or trajectory, such as a single starting point, a few initial observations, or randomly obstructed sequences. By merging these two modalities, we can harness the high accuracy of computer vision tasks and the accessibility and low computational resource consumption of mobile computing. Our approach utilizes a denoising diffusion model to denoise the mobile modality and transform it into layout sequences.

In the denoising diffusion model (LTrajDiff), we first propose a Random Mask Strategy (RMS in Section 4.1) to simulate the random obstruction input signals. Then, we propose a Siamese Masked Encoding Module (Section 4.2) to extract the 3D layout information from limited observations with a Layout Extracting Module (LEM in Section 4.2.2) and align the inputs of mobile and visual modalities while extracting temporal information with a Temporal Alignment Module (TAM in Section 4.2.1). Finally, to better leverage the visual and mobile modalities, we propose a Modality Fusion Module (MFM in Section 4.3.1) to merge the two modalities into the diffusion model. Our method outperforms all other baselines in both extremely short observations and randomly obstructed observations, and we conduct thorough ablation studies to illustrate the function of each component module.

The contributions of this paper are as follows:

- We introduce a novel task to predict layout sequence trajectories that combine the benefits of visual and mobile modalities to overcome their limitations and improve sequence prediction accuracy from noisy mobile modality and extremely short or randomly obstructed observations from the visual modality.
- We propose a denoising diffusion model (LTrajDiff) that accurately predicts trajectory sequences from noisy data and short or randomly obstructed layout sequences, reducing

the difficulty of predicting long sequences and improving prediction accuracy.

- We propose a RMS module to simulate and adapt to obstruction observations, an MFM module, and a Siamese Masked Encoding Module consisting of TAM and LEM to extract, leverage, and merge information from visual and mobile modalities.
- We demonstrate significant improvement over existing methods, conducting extensive ablation studies to prove the efficiency of our model, indicating that our approach can be a valuable tool for predicting layout sequences from noisy data and short or severely obstructed input sequences in neural network-based applications.

2 RELATED WORKS

The problem of layout sequence prediction is situated at the intersection of trajectory prediction and vision-wireless fusion. In trajectory prediction, the goal is to forecast future object positions based on observations. Vision-wireless fusion, on the other hand, seeks to integrate mobile modalities such as mobile computing and wireless signals with computer vision to tackle visual tasks.

2.1 Vision-Wireless Fusion

Vision-Wireless Fusion aims to leverage mobile modalities to address challenges in computer vision. Previous work has demonstrated the feasibility of integrating mobile computing and wireless signals with computer vision. For example, Liu et al.[21] employed wireless trajectories to tackle challenges in person re-identification, such as variations in pedestrian postures and clothing. Papaioannou et al.[29] used radio and magnetic maps to address camera instability and changes in field of view when tracking people in dynamic industrial settings. Additionally, Alahi et al. [2] enriched the RGB-D camera modality with mobile modalities to improve localization accuracy by estimating distance using wireless signals from individuals' cell phones. Although these works successfully integrated mobile modalities into computer vision tasks, they have received less attention in solving the problem of layout sequence prediction. In this work, we aim to explore the potential of vision-wireless fusion to address the challenges of layout sequence prediction.

2.2 Trajectory Prediction

Our work is the first to focus on layout sequence prediction, and while there are no prior works directly related to our task, trajectory prediction is a closely related topic. The objective of trajectory prediction is to forecast the future positions of objects based on a sequence of observations. Trajectory prediction can be categorized into two types: those based on wireless mobile computing and those based on computer vision.

2.2.1 Trajectory Prediction Based on Wireless Sensors. Wireless mobile computing-based trajectory prediction uses only data from wireless sensors as input and estimates the relative locations of mobile devices using the noisy sensor data. For example, Liu et al.[20] use Kalman filtering techniques to estimate the movement behavior of mobile users for trajectory prediction, which helps manage the rerouting and mobile handoff in wireless ATM networks management. Mlika et al.[24] propose to use quantum reservoir computing

to predict mobile users' trajectories in mobile wireless networks to address mobility management problems in self-organizing and autonomous 6G networks. Gao et al. [8] propose a method of fingerprint location for Wi-Fi signals assisted by smartphone built-in sensors to improve the location accuracy and reduce the adverse effects of environmental factors. However, these trajectory prediction methods purely based on mobile modality suffer from the limitations of the sensors, which results in inaccurate and limited information. The strength of wireless signals is used to estimate the distance between the receiver and communication devices like smartphones, and IMU or other sensors capture the movement or speed information of users, or GPS locations are used, which cannot be used in outdoor locations. Therefore, the acquired information is often too noisy and inaccurate.

2.2.2 Trajectory Prediction Based on Computer Vision. In contrast, computer vision-based trajectory prediction methods analyze images, videos, graphs, point clouds, and other media to provide accurate locations. For example, Li et al.[15] use graph-based transformers to model historical trajectory with a memory graph to smooth and predict multiple trajectories. Liang et al.[17] predict pedestrian future paths/ trajectories from videos by modeling their interaction between human behaviors and surroundings. Qian et al.[31] propose a method in an "easy-to-hard" schema to hierarchically divide the model into inter-trajectory view and intra-trajectory level. Ye et al.[36] propose a temporal point cloud learning network to capture spatial and temporal information and perform trajectories prediction directly from point cloud. However, computer vision-based trajectory prediction methods are limited by restricted scenarios, limited field of view, and obstruction, which greatly limit real-world applications, and many works are confined to indoor scenarios with a good viewpoint that can see every object, such as sports events.

2.2.3 Layout Sequences Prediction Based on Combination of Visual and Mobile Modality. To overcome the limitations of the wireless sensor-based trajectory prediction methods and the problems of restricted scenarios, limited field of view, and obstruction in computer vision-based trajectory prediction, we propose to combine mobile and visual modalities to solve the layout sequence prediction problem. We do not directly work on trajectory prediction because layout sequence prediction requires object size, spatial information, and projection status, which are more challenging but more meaningful to solve. Our novel approach aims to fuse the strengths of both visual and mobile modalities to enhance the accuracy and reliability of layout sequence predictions in complex real-world scenarios. By leveraging the high accuracy of computer vision tasks and the accessibility and low computational resource consumption of mobile computing, we hope to pave the way for more advanced solutions in the field of layout sequence prediction.

3 PROBLEM DEFINITION

We consider a set of N agents denoted by $\Omega = 1, 2, \dots, N$, observed between timestamps t_1 and t_p . The coordinate of the i -th agent at timestamp t_q is denoted by $x_i^{t_q}$. The set of coordinates between timestamps $[t_q : t_p]$ is $X_i^{t_q:t_p} = \{x_i^q, \dots, x_i^t, \dots, x_i^p\}$, where $x_t \in \mathbb{R}^2$. The layout sequence of the i -th agent at timestamp t is denoted by $l_i^t \in \mathbb{R}^5$, and the mobile modality signal of the i -th agent at

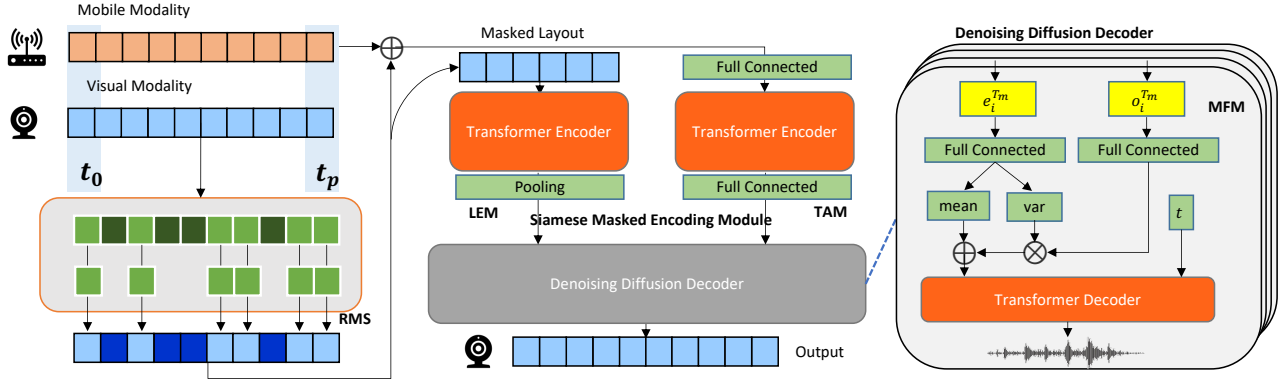


Figure 2: Overview of Our Denoising Diffusion Model (LTrajDiff). Our model takes sensor data from a mobile modality and a few timestamps of layout sequence as input, and outputs imputed 3D layout sequences in the form of projected layout information with estimated bounding box size and depth. The model comprises a diffusion model and a Siamese Masked Encoding Module to denoise noisy mobile data and predict accurate layout sequences. Leveraging object size inference, our model can generate accurate layout sequences from incomplete and noisy data, making it a promising solution for pedestrian movement prediction in real-world scenarios.

timestamp t is denoted by $s_i^t \in \mathbb{R}^{19}$. The layout sequence l_i^t consists of a bounding box $b_i^t \in \mathbb{R}^4$ and a depth value $d_i^t \in \mathbb{R}^1$. The mobile modality signal includes IMU sensor data sequences and Wi-Fi sensor data sequences. To simulate missing observations due to obstructions or out of sight of cameras, we define a mask matrix $M_i^{t,q:t,p} = \{m_i^q, \dots, m_i^t, \dots, m_i^p\}$, where $m_i^t \in \{0, 1\}$ represents whether the observation of the i -th agent at timestamp t is missing or not. Our task is to predict the visual layout sequence trajectory $\hat{L}_i^{t,q:t,p}$ in the camera view, given noisy mobile sensor data $S_i^{t,q:t,p}$ and a randomly obstructed and missing short visual observation. We simulate the visual observation by masking the ground truth visual sequence $L_i^{t,q:t,p}$ with the missing mask matrix $M_i^{t,q:t,p}$, which yields the input visual sequence $I_i^{t,q:t,p}$:

$$I_i^{t,q:t,p} = L_i^{t,q:t,p} \bullet M_i^{t,q:t,p}. \quad (1)$$

Formally, our goal is to learn a function $f(\cdot)$ that can predict $\hat{L}_i^{t,q:t,p}$ from $I_i^{t,q:t,p}$ and $S_i^{t,q:t,p}$:

$$\hat{L}_i^{t,q:t,p} = f(I_i^{t,q:t,p}, S_i^{t,q:t,p}). \quad (2)$$

Our approach is based on a denoising diffusion model with a masked encoding module that denoises the noisy mobile data and infers object size to predict accurate bounding box trajectories.

4 METHODOLOGY

The overall architecture of our proposed method is illustrated in Fig. 2. Our method addresses the task of predicting layout sequences by embedding noisy mobile data and incomplete layout sequences with a unified framework that predicts layout sequences.

4.1 Random Mask Strategy (RMS)

First, we use a random mask model to simulate the obstructed and out-of-sight processes in real-world scenarios. We improve on the approach used in MAE [13] by randomizing not only the position

of the mask but also the ratio of masked elements to the overall length of the input sequence. We define the mask model as follows:

$$M_i^{t,q:t,p} = \text{Shuffle}([0]_{(q-p)*r} \circ [1]_{(q-p)*(1-r)}), r \sim U(0, 1), \quad (3)$$

where **Shuffle** is a function that rearranges the indices of the mask matrix, r denotes the random mask ratio, and $U(0, 1)$ is a uniform distribution between 0 and 1. $[a]_b$ denotes a list with b elements of value a , and \circ denotes the concatenation operation between two lists.

4.2 Siamese Masked Encoding Module

In this section, we aim to address the two challenges presented in the introduction. Firstly, in Section 4.2.1, we tackle the issue of noise that is often introduced in mobile modality, which makes it difficult to extract accurate signals. Secondly, in Section 4.2.2, we handle the challenge of missing important information, such as object size and other details contained in bounding boxes, in these trajectory's signals.

Although extracting information from noisy mobile modality and predicting layout information from a limited number of timestamps is challenging, real-world scenarios demand that our model can handle both tasks simultaneously. To achieve this, we propose a pair of Siamese encoders comprising a temporal alignment module and a layout extraction module. These encoders aim to abstract the layout information and target object size and layout information.

Aiming to synchronize and align the noisy data and incomplete layout sequences, we employ a temporal alignment module to encode the concatenated feature of incomplete visual modality and noisy wireless sensor signals in the mobile modality. Meanwhile, we use a layout extraction module to encode the layout under the masked area.

4.2.1 Temporal Alignment Module (TAM). The temporal alignment module is a transformer [34] module with fully connected layers before and after. It takes the incomplete visual layout sequence

$I_i^{t_q:t_p}$ and the noisy wireless sensor signals $S_i^{t_q:t_p}$ as inputs and outputs the aligned feature embedding $E_i^{t_p:t_q}$.

The transformer module consists of multiple layers of self-attention and feed-forward neural networks. Each layer first applies a self-attention mechanism to capture the temporal dependencies between different timestamps. Then, a feed-forward neural network is used to transform the attention output, followed by a residual connection and a layer normalization operation. This process is repeated for multiple layers, and the output of the last layer is used as the temporal alignment feature embedding $e_{\text{TAM}}^{t_p:t_q}$. This process can be denoted as,

$$e_i^{t_p:t_q} = \mathbb{E}_{\text{TAM}}((L_i^{t_q:t_p} \bullet M_i^{t_q:t_p}) \oplus S_i^{t_p:t_q}), \quad (4)$$

where \oplus denotes the concatenation operation, $\hat{L}_i^{t_q:t_p}$ is the layout sequence with missing data imputed using interpolation or extrapolation methods, and \mathbb{E}_{TAM} is the temporal alignment module.

4.2.2 Layout Extracting Module (LEM). The layout extracting module aims to infer the object size, layout, and other detailed information, such as projection orientation, contained in the bounding box. To better model the layout information, the LEM takes the masked area of the visual modality as input. We use a transformer-based encoder to process the masked area, but since the masked area has a random length due to the random masked ratio, the length of the embedded feature is not fixed. To address this issue, we use a pooling layer to map the results into fixed lengths for the subsequent module to process. Formally, we denote the timestamps set T_m that are not masked as follows:

$$T_m = \{t \mid t_q \leq t \leq t_p, m_i^t = 1\}, \quad (5)$$

where the right-hand side of the notation \leq represents the condition for the timestamps set t . Then, the masked area of the visual modality $\hat{I}_i^{t_q:t_p}$ can be defined as follows:

$$\hat{I}_i^{t_q:t_p} = I_i^{T_m}, \quad (6)$$

here, $I_i^{T_m}$ is first processed by the transformer-based encoder and then fed into a pooling layer. Specifically, we apply a mean calculation on the timestamp dimension. Consequently, the embedded layout feature $o_i^{T_m}$ from LEM can be computed as follows:

$$o_i^{T_m} = \frac{1}{T} \sum_{t=1}^T \mathbb{E}_{\text{LEM}}(I_i^{T_m}), \quad (7)$$

where \mathbb{E}_{LEM} is the layout extracting module, and T is the length of the set T_m . This formula computes the mean of the feature $\mathbb{E}_{\text{LEM}}(I_i^{T_m})$ over the time dimension.

By combining the temporal alignment module (TAM) and the layout extracting module (LEM), our Siamese Masked Encoding Module can effectively synchronize and align the noisy data and incomplete layout sequences and infer the object size, layout, and other detailed information contained in the bounding box. In doing so, our model can handle the challenges of extracting information from noisy mobile modality and predicting layout information from a limited number of timestamps in complex real-world scenarios.

4.3 Denoising Diffusion Decoder

In this section, we implement a decoder based on the diffusion model to decode the features of layout representation and temporal alignment representation. The diffusion model is a powerful generative model capable of handling a wide range of data distributions and generating high-quality samples. We use a coarse-to-fine diffusion model to gradually remove noise and synthesize the predicted layout sequence. In particular, the diffusion model allows us to iteratively refine the noisy input data and generate a denoised output. We adopt a diffusion model to jointly obtain embeddings from the layout feature and the temporal alignment feature.

4.3.1 Modality Fusion Module (MFM). Let $e_i^{t_p:t_q}$ denote the temporal alignment feature embedding for node i from time step t_p to time step t_q , and let $o_i^{T_m}$ denote the embedded layout feature for node i at time step T_m . First, we use the fully-connected layer f to map the temporal alignment feature embedding $e_i^{t_p:t_q}$ to the mean μ and variance σ of the normal distribution:

$$\mu, \sigma = f(e_i^{t_p:t_q}). \quad (8)$$

Next, we use the fully-connected layer g to map the embedded layout feature $o_i^{T_m}$ to a modality fusion feature z_i :

$$z_i = \sigma \bullet g(o_i^{T_m}) + \mu. \quad (9)$$

4.3.2 Diffusion Model. The diffusion model is implemented with a transformer decoder. In the k -th iteration, the transformer decoder takes the modality fusion feature z_i , time embedding t , and a noisy layout sequence by adding noise in the forward process ϵ from $L_i^{t_q:t_p}$ to predict the noise item $\hat{\epsilon}$ in the backward process in the diffusion model. The forward process of the diffusion model is,

$$y_k = \sqrt{a_k} y_0 + \sqrt{1 - a_k} \epsilon, \quad (10)$$

where y_k is the k -th output of the diffusion model, so $y_0 = L_i^{t_q:t_p}$. $\epsilon = \mathcal{N}(0, 1)$. $a_t = 1 - \beta_t$, where a_t is calculated from a variance schedule $\beta_t \in (0, 1)_{t=1}^T$ which is an equivariant series that controls the step sizes of the diffusion model. The reverse process of the diffusion model can be denoted as,

$$\hat{\epsilon} = \mathcal{F}(z_i, t, y_{k-1}), \quad (11)$$

in which \mathcal{F} is the transformer decoder. So, the loss function will be,

$$\mathcal{L} = \lambda \mathcal{L}_2(\hat{\epsilon} - \epsilon), \quad (12)$$

in which the \mathcal{L}_2 is the L2 loss function, and λ is the weighting coefficients.

4.3.3 Training. The denoising diffusion decoder is trained from scratch through iterative steps. The model performs a single iteration of the denoising diffusion process in each training step. During training, we sample a random diffuse step between $[0, K]$, where K represents the total number of iterations. In each iteration, the model aims to predict the noise introduced in that diffusion step to reveal the potential signal for the next denoising step. During testing, the model is initially fed with a randomly sampled noise from a normal distribution in the first iteration. The predicted denoised vector from each iteration is then added to the predicted results of the previous iteration in the subsequent iteration. This iterative process is repeated K times until we obtain the final results.

4.4 Implementation Details

In this section, we provide detailed information about the implementation of our method. We use the Adam [14] optimizer to jointly train the entire model. The learning rate is set to $1e-3$. An exponential learning rate decay scheduling is applied, with the learning rate decaying exponentially by multiplying a gamma value of 0.98. We use two NVIDIA RTX 2080Ti GPUs with 11 GB CUDA memory for training. The batch size for training is set to 256.

5 EXPERIMENTS

5.1 Datasets

We evaluate our method on two datasets, the Vi-Fi Multi-modal Dataset [18, 19] and the H3D Dataset [30], for the problem of layout sequence prediction from noisy mobile data. To assess our proposed method, we require datasets that contain layout sequences (trajectories, bounding boxes, depths, etc.) in the vision modality and wireless sensor signals (IMU, GPS, and other sensor signals) in the mobile modality. Please refer to the details of the datasets in Appendix. ??.

5.2 Metrics

Since our work is the first to focus on the task of layout sequence (trajectories, bounding box, depth) prediction, we cannot directly use the metrics from trajectory prediction tasks. We need new metrics to better evaluate our task. Please note that our layout sequences are in the form of concatenated left-bottom coordinates and width, height, and depth of the bounding box.

5.2.1 Mean Square Error per Timestamp (MSE-T). We calculate the Mean Square Error between two layout sequences, ignoring spatial relationships for simplicity. The result is an average over the timestamp dimension. The formula can be denoted as:

$$\mathcal{L}_{MSE-T} = \frac{1}{T} \sum_{t=1}^T \left| L_i^{t_q:t_p} - \hat{L}_i^{t_q:t_p} \right|^2, \quad (13)$$

here, \mathcal{L}_{MSE-T} is the calculated MSE-T metric. T is the length between $t_q : t_p$. $L_i^{t_q:t_p}$ and $\hat{L}_i^{t_q:t_p}$ are the visual layout sequence trajectory and its ground truth.

5.2.2 Intersection over Union with Depth (IoU-D). Because the predicted layout sequence contains depth, coordinates, width, and height simultaneously, applying MSE directly ignores the spatial information between these elements. We modify the standard IoU to include depth information and better leverage width and height for our task.

$$\mathcal{L}_{IoU-D} = \frac{(l_1 * l_2)}{w * h + \hat{w} * \hat{h} - l_1 * l_2} * \frac{|d - \hat{d}|}{\max(d, \hat{d})}, \quad (14)$$

here, d and \hat{d} , w and \hat{w} , and h and \hat{h} are the depth, width, and height in the predicted layout sequence and ground truth, respectively. l_1 and l_2 are the overlap areas of two bounding boxes on width and height.

5.3 Baselines

Predicting layout sequences from noisy mobile modality is a new task, so we implement four baselines with different input settings for evaluation. Note that the input for these baselines is a concatenation of the incomplete visual layout sequence and the noisy wireless sensor signals, while the output is complete visual layout sequences. As our proposed method is a diffusion-based model with only \mathcal{L}_2 loss applied, these baselines use \mathcal{L}_2 loss during training.

5.3.1 ViTag [6]. Vi-Tag is the current state-of-the-art method on the Vi-Fi dataset [18, 19] for the vision-motion identity association task, which aims to match identities in cameras in the vision modality with wireless signals in the mobile modality. The core of Vi-Tag is the X-Translator model, which translates the visual modality to the mobile modality and finds the most similar wireless signals to match the identities in both modalities. We modify the X-Translator to translate the concatenation of the incomplete visual layout sequence and the noisy wireless sensor signals into complete visual layout sequences.

5.3.2 UNet [32]. UNet is a well-known auto-encoder backbone architecture widely used in various research topics, including image segmentation, generative models, action recognition, and trajectory prediction. To adapt it to our task, we need to reshape the input and output into 2D images. Despite its excellent performance in these tasks, the main drawback of UNet is that it requires input and output to have a fixed shape and cannot process data with variable lengths.

5.3.3 Other Seq2seq Models. We also adapt other sequence-to-sequence models originally designed for trajectory prediction-related tasks, such as LSTM [33] and Transformer [9]. The models are implemented as encoder-decoder architectures. The inputs are synchronized on the dimension of timestamps before being fed into the seq2seq model.

5.4 Quantitative Comparison Experiments (randomly obstructed experiments)

In this section, we present the quantitative experiments, with details of the implemented baselines listed in Section 5.3.

As shown in Table 1, under the random visibility mask with a random ratio setting, the results on the MSE-T dataset are relatively high. The H3D dataset shows better overall MSE-T scores because it has more mobile modality sensors. This provides more data sources and dimensions that can partly eliminate the noise in the mobile modality, helping the model learn better movement cues to recover the movement status and ultimately lead to better layout sequences. Among the baselines, except for our model yielding the best results, the UNet [32] and Transformer [9] also perform well in terms of the MSE-T metric on the Vi-Fi dataset. However, their IoU-D results are worse than ours, as are the MSE-T results on the H3D dataset.

5.5 Extremely Short Input Experiments

As shown in Table 2, our model outperforms the baselines in the extremely short input experiments without the Phase-I and Phase-II training schemes. The second-best baseline, UNet, also achieves good results in this experiment, while LSTM and Vi-Tag do not.

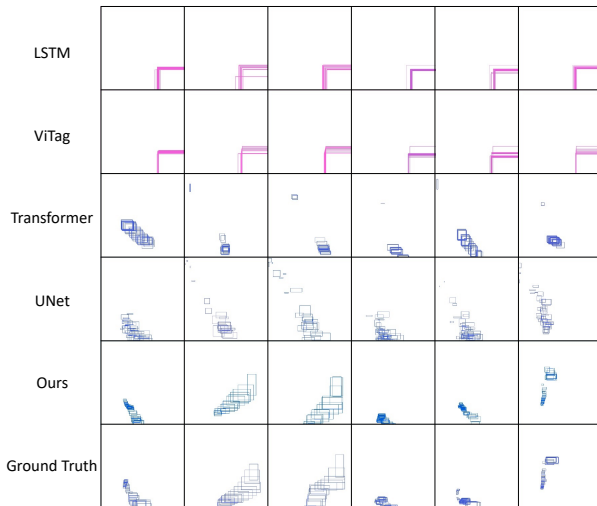


Figure 3: Comparison of Visualization Results. The figure above provides a visual comparison of the predicted layout sequences generated by different methods. Each method’s predicted layout sequence is presented, and the corresponding objects are depicted as rectangles representing their bounding boxes. The color of each bounding box reflects the depth of the object, with darker blue shades indicating closer proximity. It is worth noting that in the first and second rows, the LSTM and ViTag methods encounter difficulties in converging on this task, as evidenced by their less accurate predictions. For the purpose of comparison, only the outputs are displayed in this figure.

| Dataset Metrics | H3D [30] | Vi-Fi [18] | |
|------------------|----------|------------|---------|
| | MSE-T ↓ | MSE-T ↓ | IoU-D ↑ |
| LSTM [33] | 452.14 | 432.33 | 0.04 |
| ViTag [6] | 455.61 | 421.42 | 0.04 |
| Transformer [9] | 5.17 | 58.29 | 0.42 |
| UNet [32] | 5.92 | 58.79 | 0.43 |
| MID [11] | 13.48 | 64.07 | 0.18 |
| HIVT [37] | 2.88 | 66.07 | 0.19 |
| LTrajDiff (Ours) | 2.72 | 56.13 | 0.69 |

Table 1: Evaluation of the Denoising Diffusion Model against Baseline Approaches on H3D and Vi-Fi Datasets with Two Metrics. Compared to other baselines adapted to random length and random visibility masks, our proposed model achieves superior performance in terms of MSE-T and IoU-D. Note that the layout sequences in the H3D dataset are not bounding boxes (objects with mobile signals are not annotated with a bounding box), so we can only apply MSE-T for evaluation.

This experiment showcases the ability to predict with extremely short inputs.

| Model | Phase-I ↓ | Phase-II ↓ |
|-----------------|-----------|------------|
| LSTM [33] | 110.11 | 116.24 |
| ViTag [6] | 110.30 | 110.32 |
| Transformer [9] | 28.28 | 28.27 |
| UNet [32] | 3.42 | 5.52 |
| HIVT [37] | - | 17.51 |
| MID [11] | - | 13.32 |
| LTrajDiff(Ours) | - | 4.48 |

Table 2: Evaluation on Extremely Short Inputs of Our Model Against Baseline Approaches. Phase-I indicates when input has 10/50 of the predicted length, while Phase-II indicates the input has 1/50 of the predicted length. Compared to other baselines that require a Phase-I and Phase-II training strategy to adapt to extremely short input sequences (only one timestamp), our proposed model achieves superior performance in terms of MSE-T. Note that the ↑ means high is better and the ↓ means low is better.

5.6 Visualization Results

The visualization results are shown in Fig.3. Upon observing the results, it becomes evident that both ViTag and LSTM encounter difficulties in converging on this task, resulting in inconsistent and inaccurate predicted layout sequences. On the other hand, Transformer and UNet exhibit the ability to approximate the trajectory and depth to some extent, but they struggle with accurately inferring the size of the bounding boxes. In contrast, our proposed model showcases superior performance by accurately predicting a rectangular box trajectory with precise bounding box sizes. This highlights the effectiveness of our method in addressing the challenges associated with layout sequence prediction.

5.7 Ablation Study of Modules

In this experiment, we remove each component module in our model to demonstrate the functions of each module. The results of the experiments are shown in Table 3. We will introduce the settings of the experiment and analyze the results in this section.

As shown in Table 3, the performance drops if we remove any of the module elements. Specifically, removing the MFM module causes both metrics to drop slightly, but it remains better than other ablations. This indicates that MFM helps the model better fuse the features from TAM and LEM. Without MFM, the performance drops due to difficulty in modality fusion. Removing the LEM module causes a slight drop in MSE-T but leads to a significant drop in IoU-D, which indicates that the LEM module has a strong relationship with IoU-D. This means that LEM plays a role in extracting layout spatial information to help the model predict better 3D layouts in bounding boxes and depth. Without the TAM module, the performance of both MSE-T and IoU-D degrades because it is difficult for the model to make predictions if temporal information is lost. The relationship between LEM and TAM is that TAM helps the model understand spatial information, but without TAM to provide temporal alignment information to the model, both performances degrade. These results demonstrate the efficiency of TAM and reveal the relationship within the Siamese Masked Encoding Module.

| Model Variant | MSE-T ↓ | IoU-D ↑ |
|-----------------|---------|---------|
| w/o RMS (4.1) | 307.41 | 0.08 |
| w/o MFM (4.3.1) | 113.55 | 0.45 |
| w/o TAM (4.2.1) | 295.93 | 0.15 |
| w/o LEM (4.2.2) | 64.07 | 0.18 |
| Complete model | 56.13 | 0.69 |

Table 3: Ablation Study of Model Components. We removed individual modules from our complete model (corresponding subsections in the Method Section are listed in brackets). The results demonstrate that the IoU-D metric experiences a significant drop when the TAM and LEM modules are excluded, while MSE-T decreases substantially when the TAM or MFM module (responsible for processing the features from TAM and LEM) is removed. Without the RMS module, the performance is poor. Note that the ↑ signifies higher values are better and the ↓ indicates lower values are better.

The poor performance of "w/o RMS" indicates that the model will have out-of-distribution issues because the inputs during training and testing will be too different for the model to adapt. This result shows that RMS can simulate incomplete testing samples to aid model training.

5.8 Ablation Study of Modality

This experiment aims to determine the contributions of visual and mobile modalities in helping the model predict layout sequences.

5.8.1 Experiments Setup. To isolate the modality, for each modality, we completely remove the incomplete layout sequences (in visual modality) or noisy mobile sensor data sequences (in mobile modality). Although we attempt to keep the architecture unchanged when training with a single modality, the LAM module takes only the unmasked area in incomplete layout sequences as input. As a result, we remove the LAM module when implementing the "w/o Visual Modality", and the TAM module only takes the noisy mobile sensor data sequences (in mobile modality). In the implementation of "w/o Mobile Modality", we simply remove the noisy mobile sensor data sequences (in mobile modality) from the input of the TAM module.

5.8.2 Results Analysis. As shown in Table 4, when either visual or mobile modality is removed from the inputs, the model's performance declines significantly. This indicates that both modalities are crucial for the layout prediction process. Furthermore, the similar drops in performance for both MSE-T and IoU-D metrics suggest that the two modalities, as well as the extracted spatial layout information and temporal alignment information, have comparable levels of importance in layout sequence prediction.

6 LIMITATION DISCUSSION

The main distinction in computation lies in the inclusion of additional dimensions, such as depth, x and y coordinates, height, and width of the bounding box, compared to traditional trajectory prediction. However, in terms of time cost, there is no significant difference between layout sequence prediction and trajectory prediction. Both tasks involve predicting coordinates and dimensions,

| Modality Variant | MSE-T ↓ | IoU-D ↑ |
|--------------------------|---------|---------|
| w/o Mobile Modality | 387.86 | 0.29 |
| w/o Visual Modality | 362.33 | 0.33 |
| Mobile + Visual Modality | 56.13 | 0.69 |

Table 4: Ablation Study of Input Modality. Our model's performance is greatly impacted when either the visual or mobile modality is removed from the input. Results on both MSE-T and IoU-D metrics drop significantly without both modalities as inputs. This experiment confirms the importance of both modalities in the layout prediction process. Note that the ↑ means high is better and the ↓ means low is better.

and the additional dimensions in layout sequences prediction do not significantly impact the computational complexity.

That being said, while our LTrajDiff achieves remarkable performance, the diffusion model requires forwarding K times to predict the final layout sequences during the testing process, which can be time-consuming. One potential avenue to mitigate this limitation is to explore deep learning acceleration techniques and model pruning methods for the diffusion model, which can significantly reduce the inference time. Additionally, future researchers could investigate alternative models that strike a balance between accuracy and acceleration. Furthermore, our current model provides a projection of the bounding box with depth information. However, there is room for improvement by incorporating real-time volume segmentations or 3D mesh representations to gather more comprehensive information. We will discuss these potential avenues to highlight the future directions of research in our conclusion.

7 CONCLUSION

Our study addresses a prevalent issue in real-world scenarios, where inputs are often assumed to be unobstructed, complete, and accurate camera trajectory sequences. We introduce a novel approach that leverages noisy mobile modality data to consider objects that are out-of-sight or obstructed by complex environments. To overcome the challenges associated with noisy mobile modalities, we propose a denoising diffusion model. Specifically, we introduce the Modality Fusion Module to tackle modality fusion challenges, the Siamese Masked Encoding Module to leverage information from both visual and mobile modalities to address noisy data issues, and the Layout Extracting Module to handle missing spatial layout and object size information. Through experiments, we demonstrate the efficiency and superiority of our architecture and contributions. Our model achieves state-of-the-art performance. This demonstrates the effectiveness of our approach in leveraging noisy mobile data to predict layout sequences. To the best of our knowledge, this is the first work to address severely obstructed and extremely short input layout sequences by leveraging the combination of computer vision and noisy mobile modality. Our findings pave the way for further research and development in the fusion of diverse data sources to tackle real-world challenges.

8 ACKNOWLEDGEMENT

This research was sponsored by Toyota Motor North America.

REFERENCES

- [1] Moustafa Abbas, Moustafa Elhamshary, Hamada Rizk, Marwan Torki, and Moustafa Youssef. 2019. WiDeep: WiFi-based accurate and robust indoor localization system using deep learning. In *2019 IEEE International Conference on Pervasive Computing and Communications (PerCom)*. IEEE, 1–10.
- [2] Alexandre Alahi, Albert Haque, and Li Fei-Fei. 2015. RGB-W: When vision meets wireless. In *Proceedings of the IEEE International Conference on Computer Vision*. 3289–3297.
- [3] Ali Reza Amiri-Simkooei, Christian CJM Tiberius, and Peter JG Teunissen. 2007. Assessment of noise in GPS coordinate time series: methodology and results. *Journal of Geophysical Research: Solid Earth* 112, B7 (2007).
- [4] Axel Barrau and Silvere Bonnabel. 2020. A mathematical framework for IMU error propagation with applications to preintegration. In *2020 IEEE International Conference on Robotics and Automation (ICRA)*. IEEE, 5732–5738.
- [5] Nicola Barthelme, Stefan Sicklinger, and Markus Zimmermann. 2022. The impact of the camera setup on the visibility rate of traffic lights. In *2022 IEEE International Conference on Multisensor Fusion and Integration for Intelligent Systems (MFI)*. IEEE, 1–6.
- [6] Bryan Bo Cao, Abrar Alali, Hansi Liu, Nicholas Meegan, Marco Gruteser, Kristin Dana, Ashwin Ashok, and Shubham Jain. 2022. ViTag: Online WiFi Fine Time Measurements Aided Vision-Motion Identity Association in Multi-person Environments. In *2022 19th Annual IEEE International Conference on Sensing, Communication, and Networking (SECON)*. IEEE, 19–27.
- [7] Tobias Ehlgen, Tomas Pajdla, and Dieter Ammon. 2008. Eliminating blind spots for assisted driving. *IEEE Transactions on Intelligent Transportation Systems* 9, 4 (2008), 657–665.
- [8] Kun Gao, Hao Wang, Joanicjusz Nazarko, and George Chobanov. 2021. Indoor Trajectory Prediction Algorithm Based on Communication Analysis of Built-In Sensors in Mobile Terminals. *IEEE Sensors Journal* 21, 22 (2021), 25234–25242. <https://doi.org/10.1109/JSEN.2021.3058141>
- [9] Francesco Giuliani, Irtiza Hasan, Marco Cristani, and Fabio Galasso. 2021. Transformer networks for trajectory forecasting. In *2020 25th international conference on pattern recognition (ICPR)*. IEEE, 10335–10342.
- [10] Domenico Giustiniano, Theodoros Bourchas, Maciej Bednarek, and Vincent Lenders. 2015. Deep inspection of the noise in wifi time-of-flight echo techniques. In *Proceedings of the 18th ACM International Conference on Modeling, Analysis and Simulation of Wireless and Mobile Systems*. ACM, 5–12.
- [11] Tianpei Gu, Guangyi Chen, Junlong Li, Chunze Lin, Yongming Rao, Jie Zhou, and Jiwen Lu. 2022. Stochastic Trajectory Prediction via Motion Indeterminacy Diffusion. In *Proceedings of the IEEE/CVF Conference on Computer Vision and Pattern Recognition*. 17113–17122.
- [12] Shipeng Han, Zhen Meng, Xingcheng Zhang, and Yuepeng Yan. 2021. Hybrid deep recurrent neural networks for noise reduction of MEMS-IMU with static and dynamic conditions. *Micromachines* 12, 2 (2021), 214.
- [13] Kaiming He, Xinlei Chen, Saining Xie, Yanghao Li, Piotr Dollár, and Ross Girshick. 2022. Masked autoencoders are scalable vision learners. In *Proceedings of the IEEE/CVF Conference on Computer Vision and Pattern Recognition*. 16000–16009.
- [14] Diederik P. Kingma and Jimmy Ba. 2015. Adam: A Method for Stochastic Optimization. In *3rd International Conference on Learning Representations, ICLR 2015, San Diego, CA, USA, May 7–9, 2015, Conference Track Proceedings*, Yoshua Bengio and Yann LeCun (Eds.). <http://arxiv.org/abs/1412.6980>
- [15] Lihuan Li, Maurice Pagnucco, and Yang Song. 2022. Graph-Based Spatial Transformer With Memory Replay for Multi-Future Pedestrian Trajectory Prediction. In *Proceedings of the IEEE/CVF Conference on Computer Vision and Pattern Recognition (CVPR)*. 2231–2241.
- [16] Shigang Li and Ying Hai. 2010. Easy calibration of a blind-spot-free fisheye camera system using a scene of a parking space. *IEEE Transactions on Intelligent Transportation Systems* 12, 1 (2010), 232–242.
- [17] Junwei Liang, Lu Jiang, Juan Carlos Niebles, Alexander G Hauptmann, and Li Fei-Fei. 2019. Peeking into the future: Predicting future person activities and locations in videos. In *Proceedings of the IEEE/CVF conference on computer vision and pattern recognition*. 5725–5734.
- [18] Hansi Liu, Abrar Alali, Mohamed Ibrahim, Bryan Bo Cao, Nicholas Meegan, Hongyu Li, Marco Gruteser, Shubham Jain, Kristin Dana, Ashwin Ashok, et al. 2022. Vi-Fi: Associating Moving Subjects across Vision and Wireless Sensors. In *2022 21st ACM/IEEE International Conference on Information Processing in Sensor Networks (IPSN)*. IEEE, 208–219.
- [19] Hansi Liu, Abrar Alali, Mohamed Ibrahim, Hongyu Li, Marco Gruteser, Shubham Jain, Kristin Dana, Ashwin Ashok, Bin Cheng, and Hongsheng Lu. 2021. Lost and Found! associating target persons in camera surveillance footage with smart-phone identifiers. In *Proceedings of the 19th Annual International Conference on Mobile Systems, Applications, and Services*. 499–500.
- [20] Tong Liu, Paramvir Bahl, and Imrich Chlamtac. 1998. Mobility modeling, location tracking, and trajectory prediction in wireless ATM networks. *IEEE Journal on selected areas in communications* 16, 6 (1998), 922–936.
- [21] Yiheng Liu, Wengang Zhou, Mao Xi, Sanjing Shen, and Houqiang Li. 2020. Vision meets wireless positioning: Effective person re-identification with recurrent context propagation. In *Proceedings of the 28th ACM International Conference on Multimedia*. 1103–1111.
- [22] Guozheng Lu and Fu Zhang. 2019. IMU-based attitude estimation in the presence of narrow-band noise. *IEEE/ASME Transactions on Mechatronics* 24, 2 (2019), 841–852.
- [23] Ailin Mao, Christopher GA Harrison, and Timothy H Dixon. 1999. Noise in GPS coordinate time series. *Journal of Geophysical Research: Solid Earth* 104, B2 (1999), 2797–2816.
- [24] Zoubier Mlika, Soumaya Cherkaoui, Jean Frédéric Laprade, and Simon Corbeil-Letourneau. 2023. User Trajectory Prediction in Mobile Wireless Networks Using Quantum Reservoir Computing. *arXiv preprint arXiv:2301.08796* (2023).
- [25] Anca Morar, Alin Moldoveanu, Irina Mocanu, Florica Moldoveanu, Ion Emilian Radoi, Victor Asavei, Alexandru Gradinaru, and Alex Butean. 2020. A comprehensive survey of indoor localization methods based on computer vision. *Sensors* 20, 9 (2020), 2641.
- [26] Gabriella Musarra, Piergiorgio Caramazza, Alex Turpin, Ashley Lyons, Catherine F Higham, Roderick Murray-Smith, and Daniele Faccio. 2019. Detection, identification, and tracking of objects hidden from view with neural networks. In *Advanced Photon Counting Techniques XIII*, Vol. 10978. SPIE, 1097803.
- [27] K Nirmal, AG Sreejith, Joice Mathew, Mayuresh Sarpotdar, Ambily Suresh, Ajin Prakash, Margarita Safonova, and Jayant Murthy. 2016. Noise modeling and analysis of an IMU-based attitude sensor: improvement of performance by filtering and sensor fusion. In *Advances in Optical and Mechanical Technologies for Telescopes and Instrumentation II*, Vol. 9912. SPIE, 2138–2147.
- [28] Shayegan Omidshafiei, Daniel Hennes, Marta Garnelo, Eugene Tarassov, Zhe Wang, Romuald Elie, Jerome T Connor, Paul Muller, Ian Graham, William Spearman, et al. 2021. Time-series imputation of temporally-occluded multiagent trajectories. *arXiv preprint arXiv:2106.04219* (2021).
- [29] Savvas Papaioannou, Hongkai Wen, Zhuoling Xiao, Andrew Markham, and Niki Trigoni. 2015. Accurate positioning via cross-modality training. In *Proceedings of the 13th ACM Conference on Embedded Networked Sensor Systems*. 239–251.
- [30] Abhishek Patil, Srikanth Malla, Haiming Gang, and Yi-Ting Chen. 2019. The H3D Dataset for Full-Surround 3D Multi-Object Detection and Tracking in Crowded Urban Scenes. In *International Conference on Robotics and Automation*.
- [31] Tangwen Qian, Yongjun Xu, Zhao Zhang, and Fei Wang. 2022. Trajectory Prediction from Hierarchical Perspective. In *Proceedings of the 30th ACM International Conference on Multimedia*. 6822–6830.
- [32] Luca Rossi, Marina Paolanti, Roberto Pierdicca, and Emanuele Frontoni. 2021. Human trajectory prediction and generation using LSTM models and GANs. *Pattern Recognition* 120 (2021), 108136.
- [33] Zhiyuan Shi, Min Xu, Quan Pan, Bing Yan, and Haimin Zhang. 2018. LSTM-based flight trajectory prediction. In *2018 International joint conference on neural networks (IJCNN)*. IEEE, 1–8.
- [34] Ashish Vaswani, Noam Shazeer, Niki Parmar, Jakob Uszkoreit, Llion Jones, Aidan N Gomez, Lukasz Kaiser, and Illia Polosukhin. 2017. Attention is all you need. *Advances in neural information processing systems* 30 (2017).
- [35] Chaoyang Wang, Xiaonan Wang, Hao Hu, Yanxue Liang, and Gang Shen. 2022. On the Application of Cameras Used in Autonomous Vehicles. *Archives of Computational Methods in Engineering* 29, 6 (2022), 4319–4339.
- [36] Maosheng Ye, Tongyi Cao, and Qifeng Chen. 2021. TPCN: Temporal Point Cloud Networks for Motion Forecasting. In *Proceedings of the IEEE/CVF Conference on Computer Vision and Pattern Recognition (CVPR)*. 11318–11327.
- [37] Zikang Zhou, Luyao Ye, Jianping Wang, Kui Wu, and Kejie Lu. 2022. HiVT: Hierarchical Vector Transformer for Multi-Agent Motion Prediction. In *Proceedings of the IEEE/CVF Conference on Computer Vision and Pattern Recognition (CVPR)*.